Electronic structure and deep impurity levels in structure-modulated zinc-blende–wurtzite semiconductor superlattices

Shang Yuan Ren
Department of Physics, University of Notre Dame, Notre Dame, Indiana 46556
and Department of Physics, University of Science and Technology of China, Hefei, Anhui, China*

John D. Dow
Department of Physics, University of Notre Dame, Notre Dame, Indiana 46556
(Received 28 November 1988)

A structure-modulated superlattice is a layered material whose alternate layers are composed of materials with different crystal structures. Structure-modulated superlattices can be fabricated which have no composition modulation: for example, the zinc-blende–wurtzite CdS semiconducting superlattice. We present a theory of such zinc-blende–wurtzite structure-modulated superlattices, and find the following for a nearest-neighbor tight-binding model with ideal wurtzite c/a ratio: (i) The fundamental band gap of the superlattice equals those of both the zinc-blende and the wurtzite parent structures; (ii) in the superlattice growth direction, the dispersion relations $E_n(\mathbf{k})$ for the electrons and holes are the same as in the parent materials; (iii) in directions perpendicular to the superlattice growth direction, the superlattice dispersion relations $E_n(\mathbf{k})$ lie near those of the parent zinc-blende and wurtzite materials, and (iv) deep-level energies are almost the same as in the parent materials. The zinc-blende–wurtzite superlattice is especially interesting, because the interface between zinc-blende and wurtzite structures is ambiguous.

I. INTRODUCTION

Man-made superlattices fall into three categories: (i) composition-modulated superlattices such as zb-GaAs/zb-AlAs (where the prefix "zb-" indicates zinc-blende), (ii) structure-modulated superlattices such as zb-CdS/*w*-CdS (where "*w*-" denotes wurtzite), and (iii) combined composition- and structure-modulated superlattices such as zb-ZnTe/*w*-ZnSe. To date, most research has focused on composition-modulated superlattices. Here we present a theory of zinc-blende–wurtzite structure-modulated superlattices, which are grown along the [111] zinc-blende direction and the wurtzite c axis[1]. It is well known that numerous II-VI compound semiconductors, such as ZnS, ZnSe, CdS, and CdSe exhibit both zinc-blende and wurtzite bulk crystal structures,[2] and hence are candidates for fabrication of zinc-blende–wurtzite superlattices. Dilute magnetic semiconductor alloys, such as $Zn_{1-x}Mn_xS$ and $Zn_{1-x}Mn_xSe$, are also potential constituents of zinc-blende–wurtzite superlattices. Here we treat the case of the CdS zinc-blende–wurtzite structure.

The zinc-blende–wurtzite superlattice has a particularly interesting topological feature in that it does not contain an unambiguous interface between the zinc-blende and wurtzite structures. For example, in Fig. 1, one may select the wurtzite layer as extending either from plane E to plane I, or from plane G to plane K, or from plane H to plane L. With any of these choices, the layer thicknesses of the wurtzite layer and the zinc-blende layer are the same.

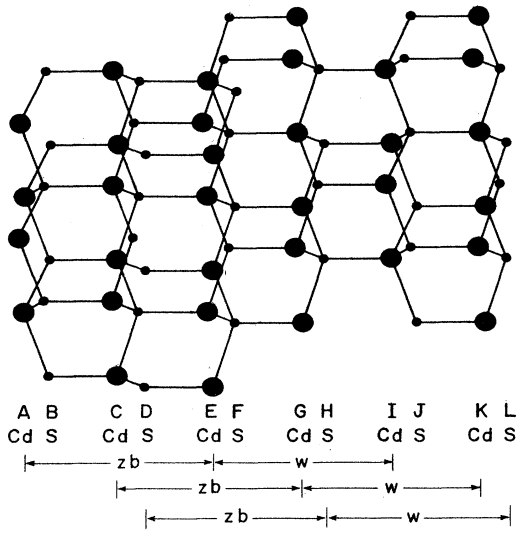

FIG. 1. Illustrating the structure of a 2×1 zinc-blende–wurtzite structure-modulated CdS superlattice with the period of two layers of zinc-blende and one layer of wurtzite structure. The large (small) circles denote Cd (S) atoms. The atomic planes are labeled $A-L$, with alternating planes containing only Cd or S atoms. The ambiguity of the zinc-blende–wurtzite interface is illustrated by noting various different layers which can be considered to be zinc-blende (zb) or wurtzite (*w*). For example, planes $A-E$ (or $C-G$, or $D-H$) can be considered to be zinc-blende, while $E-I$ (or $G-K$, or $H-L$) can be considered to be wurtzite.

II. FORMALISM

A. Host Hamiltonian

The growth direction of our CdS zinc-blende–wurtzite superlattice is defined as the direction "3" and is assumed to coincide with the zinc-blende [111] direction and the wurtzite c axis. The orthogonal directions "1" and "2" correspond to the zinc-blende $[2\,\bar{1}\,\bar{1}]$ and $[0\,1\,\bar{1}]$ direction respectively. The superlattice we consider has $N_{\rm zb}$ two-atom thick layers of zinc-blende structure and N_w four-atom thick layers of wurtzite structure repeated periodically; the zinc-blende and wurtzite structures are assumed to be perfectly lattice matched. We denote this superlattice as an $N_{\rm zb}\times N_w$ zinc-blende–wurtzite superlattice.

We first define a *superhelix* or supercell as a helical string with $2N_{\rm zb}$ adjacently bonded atoms of zinc-blende structure with its axis aligned along the [111] direction and $4N_w$ adjacently bonded atoms of wurtzite structure with its axis aligned along the wurtzite-c direction, consisting of S, Cd, S, Cd, S, Cd, . . ., S, Cd. The center of the helix is at $\mathbf{L}$ and each of the atoms of the helix is at position $\mathbf{L}+\mathbf{v}_\beta$ (for $\beta=0,1,2,\ldots,2N_{\rm zb}+4N_w-1$). A *superslab* of zinc-blende–wurtzite CdS consists of all such helixes with the same value of L_3 and all possible different values of L_1 and L_2; and the superlattice is a stacked array of these superslabs. If the origin of coordinates is taken to be at a S atom, the x and y axes are oriented such that a neighboring cation is at $(\frac{1}{4},\frac{1}{4},\frac{1}{4})a_L$, where a_L is the lattice constant of the zinc-blende structure.

We describe the electronic structure with a nearest-neighbor tight-binding Hamiltonian. At each site there are four sp^3 basis orbitals $|n,\mathbf{L},\mathbf{v}_\beta\rangle$, where $n=s$, p_x, p_y, or p_z and $\beta=0,1,2,\ldots,2N_{\rm zb}+4N_w-1$. (Because the semiconductors exhibiting both wurtzite and zinc-blende structures also have large direct gaps, it is not necessary to employ an excited s^* basis orbital at each site. Such an orbital is useful for obtaining the indirect conduction-band edges found in indirect-band-gap semiconductors.[13]) In terms of these orbitals we form the tight-binding orbitals

$$|n,\beta,\mathbf{k}\rangle=N_s^{-1/2}\sum_{\mathbf{L}}\exp(i\mathbf{k}\cdot\mathbf{L}+i\mathbf{k}\cdot\mathbf{v}_\beta)\,|n,\mathbf{L},\mathbf{v}_\beta\rangle\ , \tag{1}$$

where $\mathbf{k}$ is any wave vector of the superlattice Brillouin zone. Here N_s is the number of supercells.

The minizone wave vector is a good quantum number, and so the tight-binding Hamiltonian is diagonal in $\mathbf{k}$. Evaluation of the matrix elements $\langle n,\beta,\mathbf{k}|H|n',\beta',\mathbf{k}\rangle$ leads to a tight-binding Hamiltonian of the block tridiagonal form. For different β and β', the first three rows of block matrices are

$$\begin{bmatrix} H(0,0) & H(0,1) & 0 & \cdots & \cdots & 0 & H(0,2N_{\rm zb}+4N_w-1) \\ H^\dagger(0,1) & H(1,1) & H(1,2) & 0 & 0 & \cdots\ 0 & 0 \\ 0 & H^\dagger(1,2) & H(2,2) & H(2,3) & 0 & \cdots\ 0 & 0 \\ \vdots & \vdots & & & & & \end{bmatrix}. \tag{2}$$

The last row of blocks is

$$H^\dagger(0,2N_{\rm zb}+4N_w-1)\,0\,0\cdots0\quad H^\dagger(2N_{\rm zb}+4N_w-2,2N_{\rm zb}+4N_w-1)\quad H(2N_{\rm zb}+4N_w-1,2N_{\rm zb}+4N_w-1)\ . \tag{3}$$

Here $H(\beta,\beta')$ depends on $\mathbf{k}$ and is given in terms of various 4×4 matrices for different n and n'.

The diagonal (in β) 4×4 matrix, $H(\beta,\beta)$ at site β, is

$$H(\beta,\beta)=\langle n,\beta,\mathbf{k}|H|n',\beta,\mathbf{k}\rangle=\begin{bmatrix}\epsilon_s & 0 & 0 & 0\\ 0 & \epsilon_p & 0 & 0\\ 0 & 0 & \epsilon_p & 0\\ 0 & 0 & 0 & \epsilon_p\end{bmatrix}, \tag{4}$$

where the energies ϵ_s and ϵ_p in $H(\beta,\beta)$ are the atomic energy levels of the s and p states for the atom at the βth site, and may be obtained from tabulated parameters.[4] For a pure structure-modulated zinc-blende–wurtzite superlattice, we take the valence-band offset to be zero. That is to say, the cations and anions are assumed to have the same values of ϵ_s and ϵ_p independent of whether they lie in a zinc-blende layer or a wurtzite layer.

There are several distinct cases for which the off-diagonal (in β) matrix elements $\langle n,\beta,\mathbf{k}|H|n',\beta',\mathbf{k}\rangle$ are nonzero (for $\beta\neq\beta'$).

1. Zinc-blende intrastructure matrix elements

If β and β' both refer to nearest-neighbor sites in the zinc-blende structure, we have, for example,

$$\langle n,\beta,\mathbf{k}|H|n',\beta',\mathbf{k}\rangle=H_{c,{\rm zb};a,{\rm zb}}\ , \tag{5}$$

if β refers to a cation and β' refers to an anion. $H_{c,{\rm zb};a,{\rm zb}}$ is a 4×4 matrix whose rows and columns are labeled by n and n', which range over the values s, p_x, p_y, and p_z. Similarly we have matrix elements $H_{a,{\rm zb};c,{\rm zb}}$. These matrix elements are

$$H_{c,\mathrm{zb};a,\mathrm{zb}}=\begin{bmatrix} C_0V_1 & -C_0V_4 & -C_0V_4 & -C_0V_4 \\ C_0V_5 & C_0V_2 & C_0V_3 & C_0V_3 \\ C_0V_5 & C_0V_3 & C_0V_2 & C_0V_3 \\ C_0V_5 & C_0V_3 & C_0V_3 & C_0V_2 \end{bmatrix} . \quad (6)$$

Here we have $C_0=g_0^*$, where we have $4g_0=\exp(i\mathbf{k}\cdot\mathbf{x}_0)$, and $\mathbf{x}_0=(a_L/4)(1,1,1)$, with a_L being the lattice constant of zinc-blende CdS. Here $\mathbf{k}$ is the wave vector. In addition, we have

$$V_1=V(s,s) ,$$
$$V_2=V(x,x) ,$$
$$V_3=V(x,y) ,$$
$$V_4=V(sa,pc) ,$$

and

$$V_5=V(sc,pa) ,$$

in the notation of Vogl *et al.*,[3] and

$$H_{a,\mathrm{zb};c,\mathrm{zb}}=\begin{bmatrix} V_1(g_1+g_2+g_3) & V_4(g_1-g_2-g_3) & V_4(-g_1+g_2-g_3) & V_4(-g_1-g_2+g_3) \\ -V_5(g_1-g_2-g_3) & V_2(g_1+g_2+g_3) & V_3(-g_1-g_2+g_3) & V_3(-g_1+g_2-g_3) \\ -V_5(-g_1+g_2-g_3) & V_3(-g_1-g_2+g_3) & V_2(g_1+g_2+g_3) & V_3(g_1-g_2-g_3) \\ -V_5(-g_1-g_2+g_3) & V_3(-g_1+g_2-g_3) & V_3(g_1-g_2-g_3) & V_2(g_1+g_2+g_3) \end{bmatrix} . \quad (7)$$

We also have

$$4g_1=\exp(i\mathbf{k}\cdot\mathbf{x}_1) ,$$
$$4g_2=\exp(i\mathbf{k}\cdot\mathbf{x}_2) ,$$

and

$$4g_3=\exp(i\mathbf{k}\cdot\mathbf{x}_3) ,$$

with $\mathbf{x}_1=(a_L/4)(1,-1,-1)$, $\mathbf{x}_2=(a_L/4)(-1,1,-1)$, and $\mathbf{x}_3=(a_L/4)(-1,-1,1)$. All of the matrix elements V are those tabulated[4] for CdS.

2. *Wurtzite intrastructure matrix elements*

The wurtzite structure has an exact hexagonal symmetry, and an approximate tetrahedral short-ranged symmetry: every atom is surrounded by a near tetrahedron of four atoms of the opposite species. The nearest-neighbor geometry is tetrahedral if the wurtzite structure has the ideal c/a ratio of $(8/3)^{1/2}=1.633$. In the ideal limit, the fundamental band gap of the wurtzite crystal structure is the same as for the zinc-blende structure.[5] Most wurtzite semiconductors are very close to the ideal limit; for example, CdS, CdSe, ZnS, and ZnTe have c/a ratios of 1.632, 1.630, 1.641, and 1.637, respectively.[2] In this paper we assume that the wurtzite is ideal, with the same bond length as its zinc-blende partner. As a result, the wurtzite matrix elements, in a nearest-neighbor tight-binding model, are related to the zinc-blende matrix elements, as follows.

If β and β' both refer to nearest-neighbor sites in the wurtzite structure, we will also have

$$(n,\beta,\mathbf{k}|H|n',\beta',\mathbf{k})=H_{c,w;a,w'} . \quad (8)$$

Similarly we have matrix elements $H_{a,w;c,w}$. These matrix elements are

$$H_{c,w;a,w}=\begin{bmatrix} C_0V_1 & -C_0V_4 & -C_0V_4 & -C_0V_4 \\ C_0V_5 & C_0V_2 & C_0V_3 & C_0V_3 \\ C_0V_5 & C_0V_3 & C_0V_2 & C_0V_3 \\ C_0V_5 & C_0V_3 & C_0V_3 & C_0V_2 \end{bmatrix} . \quad (9)$$

Here the C_0 and V_i's are the same as defined before. This form is exactly the same as in (6). For the wurtzite structure we have two different forms of $H_{a,w;c,w}$ because there are four atoms in each unit cell (as opposed to two for zinc-blende); one is the same as in Eq. (7) and the other is

$$H_{a,w;c,w}=\begin{bmatrix} V_4(g_4+g_5+g_6) & V_4(-5g_4+g_5+g_6)/3 & V_4(g_4-5g_5+g_6)/3 & V_4(g_4+g_5-5g_6)/3 \\ -V_5(-5g_4+g_5+g_6)/3 & V_{21}g_4+V_{22}(g_5+g_6) & -V_{31}(g_4+g_5)+V_{32}g_6 & -V_{31}(g_4+g_6)+V_{32}g_5 \\ -V_5(g_4-5g_5+g_6)/3 & -V_{31}(g_4+g_5)+V_{32}g_6 & V_{21}g_5+V_{22}(g_4+g_6) & -V_{31}(g_5+g_6)+V_{32}g_4 \\ -V_5(g_4+g_5-5g_6)/3 & -V_{31}(g_4+g_6)+V_{32}g_5 & -V_{31}(g_5+g_6)+V_{32}g_4 & V_{21}g_6+V_{22}(g_4+g_5) \end{bmatrix} . \quad (10)$$

Here we have

$$V_{21}=(25V_{pp\sigma}+2V_{pp\pi})/27=V(x,x)+\tfrac{48}{27}V(x,y)\ ,$$

$$V_{22}=(V_{pp\sigma}+26V_{pp\pi})/27=V(x,x)-\tfrac{24}{27}V(x,y)\ ,$$

$$V_{31}=5V(x,y)/9\ ,$$

$$V_{32}=V(x,y)/9\ ,$$

$$4g_4=\exp(i\mathbf{k}\cdot\mathbf{x}_4)\ ,$$

$$4g_5=\exp(i\mathbf{k}\cdot\mathbf{x}_5)\ ,$$

and

$$4g_6=\exp(i\mathbf{k}\cdot\mathbf{x}_6)\ .$$

We also have $\mathbf{x}_4=(a_L/4)(-\frac{5}{3},\frac{1}{3},\frac{1}{3})$, $\mathbf{x}_5=(a_L/4)(\frac{1}{3},-\frac{5}{3},\frac{1}{3})$, $\mathbf{x}_6=(a_L/4)(\frac{1}{3},\frac{1}{3},-\frac{5}{3})$, and parameters V which are those tabulated[4] for CdS.

3. *Interstructure matrix elements*

The fact that the location of the zinc-blende–wurtzite interface is ambiguous means that one must (i) develop a formalism that treats the interfacial matrix elements the same, independent of interface choice, and (ii) select a specific interface for a particular calculation. There are two distinct forms for Hamiltonian matrix elements connecting one atom in the zinc-blende structure with another in the wurtzite structure. They are

$$H_{a,w;c,\mathrm{zb}}=\begin{bmatrix} V_1(g_1+g_2+g_3) & V_4(g_1-g_2-g_3) & V_4(-g_1+g_2-g_3) & V_4(-g_1-g_2+g_3) \\ -V_5(g_1-g_2-g_3) & V_2(g_1+g_2+g_3) & V_3(-g_1-g_2+g_3) & V_3(-g_1+g_2-g_3) \\ -V_5(-g_1+g_2-g_3) & V_3(-g_1-g_2+g_3) & V_2(g_1+g_2+g_3) & V_3(g_1-g_2-g_3) \\ -V_5(-g_1-g_2+g_3) & V_3(-g_1+g_2-g_3) & V_3(g_1-g_2-g_3) & V_2(g_1+g_2+g_3) \end{bmatrix} \tag{11}$$

and

$$H_{c,w;a,\mathrm{zb}}=\begin{bmatrix} V_1(C_1+C_2+C_3) & V_4(C_1-C_2-C_3) & V_4(-C_1+C_2-C_3) & V_4(-C_1-C_2+C_3) \\ -V_5(C_1-C_2-C_3) & V_2(C_1+C_2+C_3) & V_3(-C_1-C_2+C_3) & V_3(-C_1+C_2-C_3) \\ -V_5(-C_1+C_2-C_3) & V_3(-C_1-C_2+C_3) & V_2(C_1+C_2+C_3) & V_3(C_1-C_2-C_3) \\ -V_5(-C_1-C_2+C_3) & V_3(-C_1+C_2-C_3) & V_3(C_1-C_2-C_3) & V_2(C_1+C_2+C_3) \end{bmatrix}. \tag{12}$$

In the limit $N_{\mathrm{zb}}=0$, this Hamiltonian reduces to the Hamiltonian of Ref. 4 for bulk wurtzite material. In the limit $N_w=0$ it becomes the sp^3 zinc-blende Hamiltonian.[3,6] Values of the parameters for this Hamiltonian can be taken from Ref. 4 or 3.

In this work we study electronic structure for superhelices as large as $N_{\mathrm{zb}}+2N_w=20$; that is, in 40-atom-thick superslabs. The dimension of the Hamiltonian matrix at each value of $\mathbf{k}$ is $4(2N_{\mathrm{zb}}+4N_w)$, because there are four orbitals per site. We diagonalize this Hamiltonian numerically for each $\mathbf{k}$, finding its eigenvalues $E_{\gamma,\mathbf{k}}$ and, if necessary, the projections of the eigenvectors $|\gamma,\mathbf{k}\rangle$ on the $|n,\beta,\mathbf{k})$ hybrid basis: $(n,\beta,\mathbf{k}|\gamma,\mathbf{k}\rangle$. Here γ is the band index (and ranges from 1 to 160 for $N_{\mathrm{zb}}=2N_w=10$) and $\mathbf{k}$ lies within the superlattice mini-Brillouin zone.

B. Deep levels

The theory of deep levels is based on the Green's-function theory of Hjalmarson *et al.*,[7] which solves the secular equation for the deep-level energy E

$$\det[1-G(E)V]=0=\det\left[1-P\int\frac{\delta(E'-H)}{(E-E')}dE'\,V\right]. \tag{13}$$

Here V is the defect potential matrix,[7] which is zero except at the defect site and diagonal on that site (V_s,V_p,V_p,V_p) in the sp^3 local basis centered on each atom. We also have $G=(E-H)^{-1}$, where H is the host tight-binding Hamiltonian operator. The spectral density operator is $\delta(E'-H)$ and P denotes the principal-value integral over all energies. For energies E in the fundamental band gap of the superlattice, G is real.

A substitutional point defect in bulk zinc-blende CdS has tetrahedral (T_d) point-group symmetry. Each such s-and p-bonded defect normally has one s-like (A_1) and one triply degenerate p-like (T_2) deep defect level near or in the fundamental band gap. If we imagine breaking the symmetry of bulk zinc-blende CdS by making it into a zb-CdS/zb-CdS superlattice along the [111] direction, we reduce the T_d symmetry to C_{3v}. A substitutional point

defect in bulk wurtzite CdS also has C_{3v} point-group symmetry, and so in the zinc-blende–wurtzite superlattice and s- and p-bonded point defect will have C_{3v} symmetry as well and will produce two a_1 levels (one s-like, derived from the A_1 level and one T_2-derived p_σ like), and one doubly degenerate e level (p_π like).

The secular equation, Eq. (13), is reduced by the C_{3v} symmetry to the following two equations:

$$G(e;E)=V_p^{-1} \tag{14}$$

for e levels, and

$$\det \begin{vmatrix} G(s,s;E)V_s-1 & G(s,\sigma;E)V_p \\ G(\sigma,s;E)V_s & G(\sigma,\sigma;E)V_p-1 \end{vmatrix}=0 , \tag{15}$$

for a_1 levels, where we have

$$G(e;E)=\sum_{\gamma,\mathbf{k}} |(p_y,\beta,\mathbf{k}|\gamma,\mathbf{k}\rangle-(p_z,\beta,\mathbf{k}|\gamma,\mathbf{k}\rangle|^2/2(E-E_{\gamma,\mathbf{k}}) , \tag{16}$$

$$G(s,s;E)=\sum_{\gamma,\mathbf{k}} |(s,\beta,\mathbf{k}|\gamma,\mathbf{k}\rangle|^2/(E-E_{\gamma,\mathbf{k}}) , \tag{17}$$

$$G(\sigma,\sigma;E)=\sum_{\gamma,\mathbf{k}} |(p_x,\beta,\mathbf{k}|\gamma,\mathbf{k}\rangle+(p_y,\beta,\mathbf{k}|\gamma,\mathbf{k}\rangle+(p_z,\beta,\mathbf{k}|\gamma,\mathbf{k}\rangle|^2/3(E-E_{\gamma,\mathbf{k}}) , \tag{18}$$

and

$$G(s,\sigma;E)=\sum_{\gamma,\mathbf{k}} [(s,\beta,\mathbf{k}|\gamma,\mathbf{k}\rangle]\times[(p_x,\beta,\mathbf{k}|\gamma,\mathbf{k}\rangle+(p_y,\beta,\mathbf{k}|\gamma,\mathbf{k}\rangle+(p_z,\beta,\mathbf{k}|\gamma,\mathbf{k}\rangle]^*/[\sqrt{3}(E-E_{\gamma,\mathbf{k}})] . \tag{19}$$

Here $G(\sigma,s;E)$ is the Hermitian conjugate of $G(s,\sigma;E)$ and β is the site of the defect in the superlattice.

For each site β the relevant host Green's functions, Eqs. (16)–(19), are evaluated using the special points method,[8] and the secular equations (14) and (15) are solved, yielding $E(e;V_p)$ and two values of $E(a_1;V_s)$, and $E(a_1;V_p)$. The defect potential matrix elements V_s and V_p can be considered as the same as the defect potential in the zinc-blende structure.

III. RESULTS AND DISCUSSIONS

A. Superlattice band structures

Once the Hamiltonian is defined, the superlattice band structure $E_{\gamma,\mathbf{k}}$ is determined by diagonalizing it for each wave vector $\mathbf{k}$ in its Brillouin zone[9] (Fig. 2), which is the same as the wurtzite Brillouin zone, except that the $\Gamma-A$ length is reduced by a factor of $2/(N_{zb}+2N_w)$.

Provided the wurtzite structure has the ideal c/a ratio of $(8/3)^{1/2}$, the bulk zinc-blende, bulk wurtzite, and zinc-blende–wurtzite superlattice structures are physically indistinguishable when viewed only in the growth direction. The differences in three structures become apparent only when viewed along directions deviating from the growth axis. Therefore, for wave vectors $\mathbf{k}$ corresponding to the growth direction, the dispersion relations $E_n(\mathbf{k})$ and effective masses are the same as for the constituent zinc-blende and wurtzite materials. Hence zinc-blende–wurtzite superlattices made from direct-band-gap zinc-blende and (ideal c/a ratio) wurtzite materials are also direct-band-gap semiconductors with the same value of the fundamental gap at the Γ point of the Brillouin zone as the zinc-blende and the (ideal) wurtzite bulk materials: 2.60 eV for CdS. (Note that c/a for CdS is 1.632, only 0.05% different from the ideal ratio of $(8/3)^{1/2}=1.633$; hence the approximation of an ideal structure should introduce only small errors in the band structure, of order meV, the same order as found for InN.[10]) The lowest superlattice conduction band, as computed in the present model, is displayed for the 2×1 zinc-blende–wurtzite superlattice in Fig. 3; corresponding results for the highest valence band are given in Fig. 4. In the $\Gamma-A$ or [111] direction, the dispersion relations $E_n(\mathbf{k})$ are the same as for the zinc-blende or the (ideal) wurtzite bulk materials, but in the $\Gamma-M$, or $[2,\bar{1},\bar{1}]$ direction and the $\Gamma-K$, or $[0,1,\bar{1}]$, direction the superlattice band structures deviate slightly from the bulk electronic structures.

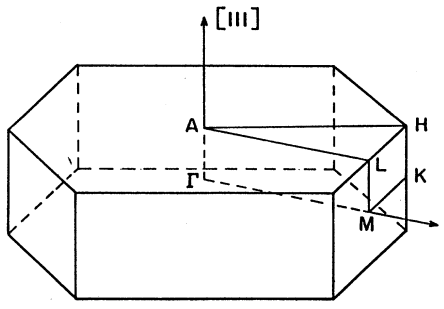

FIG. 2. The Brillouin zone for the 2×1 zinc-blende–wurtzite structure-modulated superlattice.

A quasiparticle's resistance to acceleration by an applied electric or magnetic field is determined by its effective mass. In Fig. 5 we display the calculated conduction-band and valence-band effective masses in the $\Gamma-A$, $\Gamma-M$, and $\Gamma-K$ symmetry directions, versus layer thickness of the superlattice. In our model, the conduction-band effective mass is unchanged in the superlattice, because the lowest conduction band is nondegenerate and its effective mass is isotropic for both zinc-

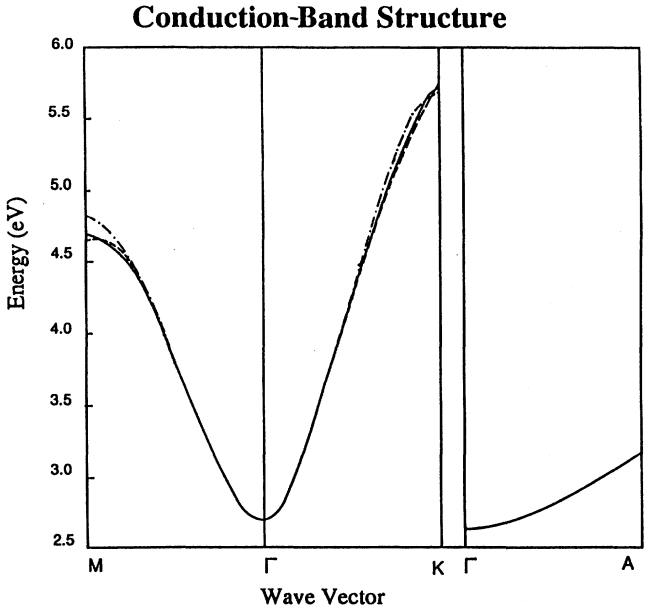

FIG. 3. The calculated lowest conduction-band structures in the three symmetry directions, $\Gamma-A$, $\Gamma-M$, and $\Gamma-K$, of the 2×1 zinc-blende–wurtzite superlattice (solid), bulk zinc-blende (dashed), and bulk wurtzite (dot-dashed) CdS. Note that the three are the same in the $\Gamma-A$ growth direction.

blende and wurtzite structures. The valence-band mass of the superlattice in the $\Gamma-A$ growth direction is independent of layer thickness and is the same as in either zinc-blende or wurtzite CdS. However, in the directions perpendicular to the growth direction, the valence-band masses change from the effective masses of wurtzite to

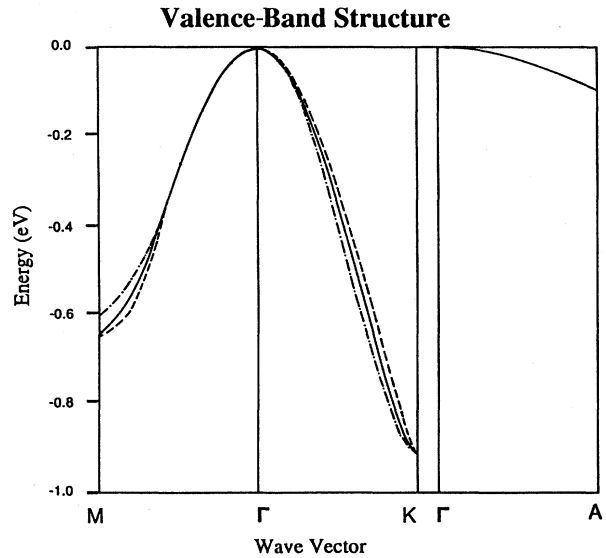

FIG. 4. The calculated highest valence-band structures in the three symmetry directions, $\Gamma-A$, $\Gamma-M$, and $\Gamma-K$, of the 2×1 zinc-blende–wurtzite superlattice (solid), bulk zinc-blende (dashed), and bulk wurtzite (dot-dashed) CdS.

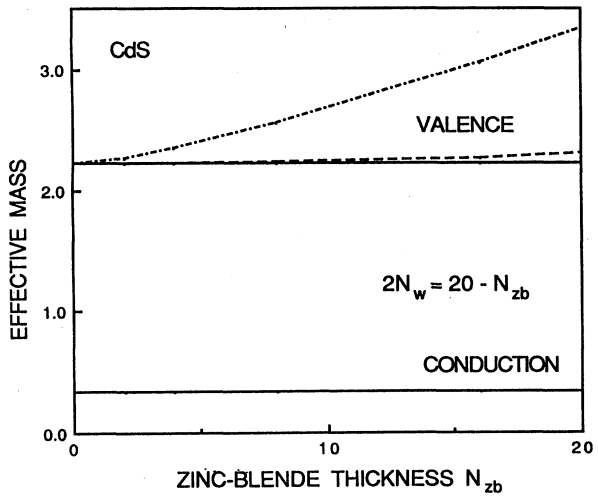

FIG. 5. The calculated reduced effective masses m^*/m_0 of the valence and conduction bands of a $N_{zb}\times N_w$ zinc-blende–wurtzite superlattice in the $\Gamma-A$ (solid), $\Gamma-M$ (dashed), and $\Gamma-K$ (dot-dashed) directions as functions of zinc-blende layer thickness N_{zb}, with $N_{zb}+2N_w=20$.

those of zinc-blende. The zinc-blende mass is anisotropic (because the valence-band maximum is triply degenerate and zinc-blende is a cubic structure) while the wurtzite mass is isotropic. The isotropy of the wurtzite valence-band mass is due to the combined effects of the lower symmetry of the wurtzite structure and the ideal c/a ratio. (For an ideal c/a ratio, the wurtzite valence-band maximum is triply degenerate, but for nonideal c/a it is nondegenerate with a doubly degenerate band slightly below it.)

B. Deep impurity levels in zinc-blende–wurtzite superlattices

Deep impurity levels are evaluated using Eq. (13) with the relevant parts of the spectral density operator $\delta(E'-H)$ expressed in terms of the Green's function (16)–(19). Since these Green's functions depend on the superlattice band structure, which differs only slightly from the bulk zinc-blende or wurtzite band structures, the deep-level energies in the CdS zinc-blende–wurtzite superlattice are virtually the same as for the same substitutional impurity in bulk zinc-blende or bulk wurtzite CdS.[11] Hence shallow-deep transitions as the layer thicknesses vary[12] are not to be expected for impurities in zinc-blende–wurtzite superlattices.

C. Long-ranged versus short-ranged order

Although the bulk zinc-blende and ideal-wurtzite structures are very different when viewed at long range, their short-ranged orders are both tetrahedral and identical (up to second-nearest neighbors). This short-ranged order leads to electronic structures of the two bulk materials that are almost identical, and to a zinc-blende–wurtzite superlattice electronic structure that is

almost the same as the bulk zinc-blende or wurtzite electronic structure. Clearly the short-ranged tetrahedral bonding, rather than any long-ranged zinc-blende, wurtzite, or superlattice order, is dominant in determining the electronic structure. While the concept of a structure-modulated superlattice is interesting, and the topology of the ambiguous zinc-blende–wurtzite interface is exciting, the practical consequences on electronic structure of growing such structures seem to be limited to introducing small anisotropies into the dispersion relations $E_n(\mathbf{k})$. In particular, such superlattices offer the possibility of introducing changes into the valence-band effective mass without significantly altering the conduction-band mass or mass isotropy.

Finally, we do expect some differences between the phonons in zinc-blende–wurtzite superlattices and the parent compounds. Although the materials will be identical when viewed along the $\Gamma - A$ (growth) direction, assuming an ideal c/a ratio, there will nevertheless be significant differences in the long-ranged Coulomb forces of zinc-blende and wurtzite structures, which should be reflected in the phonon dispersion curves.

IV. SUMMARY

The calculations presented here are, we believe, the first calculations of the electronic structures of structure-modulated semiconductor superlattices. We hope that this work will stimulate efforts to grow such interesting artificial materials.

ACKNOWLEDGMENT

We are grateful to the U.S. Air Force Office of Scientific Research (Contract No. AF-AFOSR-85-0331), Defense Advanced Research Projects Agency (Contract No. N0530-0716-09), and the U. S. Office of Naval Research (Contract No. N00014-84-K-0352) for their generous support.

---

*Permanent address.

[1]A preliminary account of this work was given by S. Y. Ren and J. D. Dow Bull. Am. Phys. Soc. **33**, 398 (1988).

[2]*Semiconductors: Physics of II-VI and I-VII Compounds, Semimagnetic Semiconductors,* Vol. 17b of *Landolt-Börnstein, Numerical Data and Functional Relationships in Science and Technology, New Series,* edited by O. Madelung, M. Schulz, and H. Weiss (Springer-Verlag, Berlin, 1982).

[3]P. Vogl, H. P. Hjalmarson, and J. D. Dow, J. Phys. Chem. Solids **44**, 365 (1983).

[4]A. Kobayashi, O. F. Sankey, S. M. Volz, and J. D. Dow, Phys. Rev. B **28**, 935 (1983).

[5]J. L. Birman, Phys. Rev. **115**, 1493 (1959), pointed out that an ideal-wurtzite semiconductor will have the same direct band gap as its zinc-blende partner.

[6]D. J. Chadi and M. L. Cohen, Phys. Status Solidi B **68**, 405 (1975).

[7]H. P. Hjalmarson, P. Vogl, D. J. Wolford, and J. D. Dow, Phys. Rev. Lett. **44**, 810 (1980).

[8]S. Y. Ren and J. D. Dow, Phys. Rev. B **38**, 1999 (1988).

[9]It may be noted that the zinc-blende structure can also have a hexagonal Brillouin zone; see S. Y. Ren and W. A. Harrison, Phys. Rev. B **23**, 762 (1981). Therefore the zinc-blende–wurtzite superlattice has a hexagonal Brillouin zone as a natural consequence.

[10]M.-H. Tsai, D. W. Jenkins, J. D. Dow, and R. V. Kasowski, Phys. Rev. B **38**, 1541 (1988).

[11]A. Kobayashi, O. F. Sankey, and J. D. Dow, Phys. Rev. B **28**, 946 (1983). In the present work we use the values β_l from Ref. 7, rather than from this reference.

[12]S. Y. Ren, J. D. Dow, and J. Shen, Phys. Rev. B **38**, 10677 (1988); R.-D. Hong, D. W. Jenkins, S. Y. Ren, and J. D. Dow, Mater. Res. Soc. Symp. Proc. **77**, 545 (1987).